ISSN 0036-0295, Russian Metallurgy (Metally), Vol. 2019, No. 4, pp. 309–314. © Pleiades Publishing, Ltd., 2019.
Russian Text © The Author(s), 2018, published in Deformatsiya i Razrushenie Materialov, 2018, No. 7, pp. 17–23.

STRUCTURE AND PROPERTIES OF THE DEFORMED STATE

Effect of a Structure and Test Conditions on the Critical Strains and Stresses in Titanium Nickelide-Based Alloys

D. E. Gusev[a], *, M. Yu. Kollerov[a], and R. E. Vinogradov[a]

[a] *Moscow Aviation Institute (National Research University), Moscow, 121552 Russia*

**e-mail: mitom@implants.ru*

Received March 26, 2018; revised March 30, 2018; accepted March 31, 2018

Abstract—The effect of the structure, the temperature, and the deformation scheme on the deformation behavior of titanium nickelide-based alloys is studied. One of the most important characteristics of the material is shown to be the temperature dependence of the critical strain corresponding to the onset of intense development of slip mechanisms.

Keywords: titanium nickelide, martensitic transformation, critical strain, critical stress, dislocation glide, structure

DOI: 10.1134/S0036029519040153

INTRODUCTION

Titanium nickelide-based alloys attract attention of material scientists and engineers due to a unique combination of their properties: a high strength, high corrosion resistance, a high damping capacity, and good biological compatibility with tissues of living organisms along with the shape memory effect (SME) and superplasticity [1–4]. These alloys are used for fabricating thermomechnical joints, thermal-force executive units, temperature sensors, and implanted medicine parts [5–7].

Studies show that the mechanical behavior of titanium nickelide-based alloys is dependent on the test temperature [1, 8], and the characteristics of SME and the superplasticity, on the strain [9–11]. Therefore, the temperature dependence of the deformation characteristic of the material should be taken into account when projecting and applying parts. It is evident that one of the most important characteristics is the limiting (critical) degree of strain, the excess of which leads to irreversible accumulation of a residual strain. It is useful to include this value in the calculations of the parts in which the accumulation of unrecovered strain during its operation is not allowable: for example, when calculating the designs of implants and actuators.

In this work, we study the effect of chemical composition, a structure, a deformation scheme, and the test temperature on the critical stresses and strains in titanium nickelide-based alloys.

EXPERIMENTAL

We carried out the studies using a wire 2.23 mm in diameter fabricated by industrial technology from ingots of two casts. Table 1 gives the chemical compositions of these alloys.

The wire was straightened out by suspending a load to one of its ends and heating by an electric current to a temperature of ≈600°C upon holding for 5 min. Then, the wire was cut into specimens about 70 mm in length. Before tests, all specimens were subjected to heat treatment, including vacuum annealing at 700°C (1 h), at which the recrystallized structure of the *B*2 phase forms [11], and two-stage aging at 500°C and 450°C. Some specimens were subjected to aging without previous annealing at 700°C. The aging regimes (the holding time at each stage) were chosen so that the temperature of the finish of shape recovery is $A_f^r = 35 \pm 1$°C. The temperatures of the onset and the finish of shape recovery (A_s^r and A_f^r) after heat treatment were determined by the technique from [12] by bending deformation of the specimens at 5°C and subsequent heating in a free state with recording the dependence of the recovered strain on the heating tempera-

Table 1. Chemical compositions of the alloys, wt %

Alloy	Ni	Ti	C	N	O	H
1	54.8	Balance	0.023	0.005	0.12	0.0017
2	55.7	Balance	0.012	0.009	0.16	0.0011

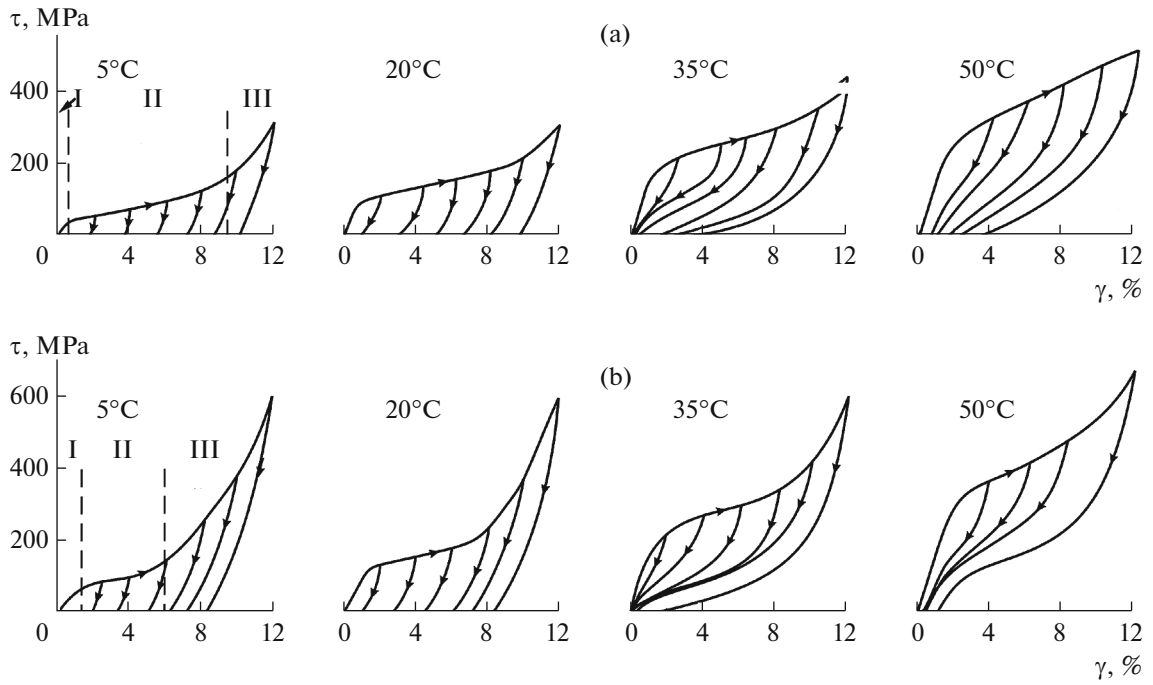

Fig. 1. Stress τ–strain γ diagrams obtained upon torsion tests at various temperatures for (a) alloy 1 and (b) alloy 2 with a recrystallized structure.

ture. The heat treated specimens were ground by tumbling and subjected by electrical polishing.

To study the thermomechanical behavior, the specimens were subjected to tension on a TIRAtest 2300 testing machine, to torsion at a UPK-1 universal torsion machine that, in its design, is an inverse torsion pendulum, and to bending by rolling around mandrels of various diameters [13]. The tests were carried out at a temperature from the range 5–50°C.

To determine the influence of deformation on the characteristics of the shape recovery, the specimens were deformed by 2–16% and, then, heated to 150°C to found the recovered and unrecovered strains. The shape recovery of the samples was carried out by heating in a water thermostat (after tension and bending) or in a tube electric furnace (after torsion) with measuring the recovered and unrecovered strains.

The critical degree of strain was used as the main characteristic determining the working capacity of these alloys. To determine this characteristic, the specimens were tested at given temperature by the loading–unloading–heating scheme in a free state with a gradual increase in the strain in each testing cycle. The total strain at which an unrecovered strain appeared in a specimen was considered as the critical strain.

Since the strains and stresses were nonunformly distributed over the specimen during tests for bending and torsion, their critical values were determined on the external specimen surface, where the strains are maximal. In spite of the fact that the stress–strain state is not favorable in homogeneity appears upon bending and torsion and, as a result, the efficiency of using of all material volume is low, the practice shows [5, 7] that it is bending and torsion that are the most widely used deformation schemes for SMA parts made from wire and sheet semifinished products.

RESULTS AND DISCUSSION

Figure 1 shows the dependence of shear stresses τ on torsion strain γ obtained as a result of torsion tests at various temperatures. According to these data, the alloys are in a plastic state at 5 and 20°C and accumulate a significant residual strain (it can be completely recovered during subsequent heating); at a temperature of 35°C or higher, the alloys demonstrate superelastic behavior [1]. It should be noted that the curves measured in specimens with recrystallized and unrecrystallized structures almost coincide.

Three characteristic segments can be separated in the τ–γ curves at the stage of loading. The first segment is related to the predominantly elastic behavior of the material. The second segment having substantially lesser slope is due to the intense formation of deformation martensite crystals and/or the reorientation of athermal martensite crystals under action of applied stresses [14]. The stress at which the transition from the first segment to the second one is observed in the stress–strain curves is the phase yield point, i.e., the martensitic shear stress (τ_m). It should be noted that the proportionality limit (τ_{pl}) and the conven-

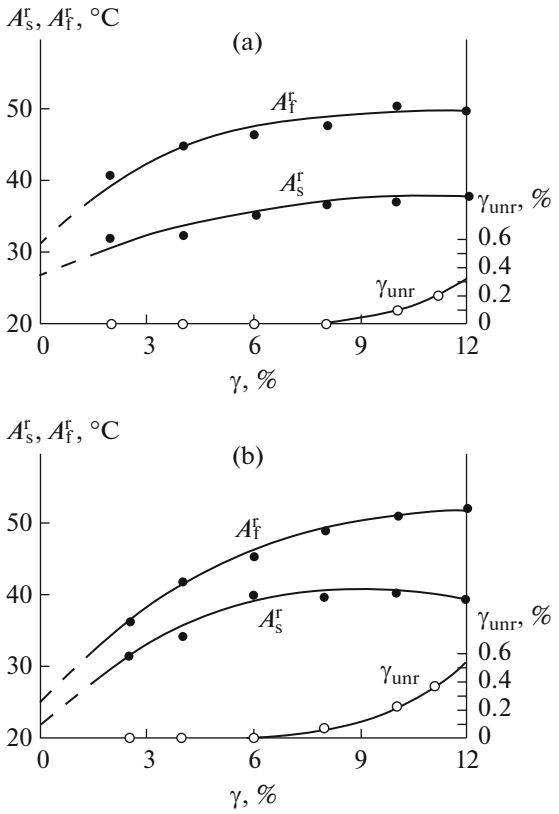

Fig. 2. Shape recovery temperatures (A_s^r, A_f^r) and unrecovered strain (γ_{ur}) vs. the torsion strain (γ) at 5°C for alloys (a) 1 and (b) 2 with a recrystallized structure.

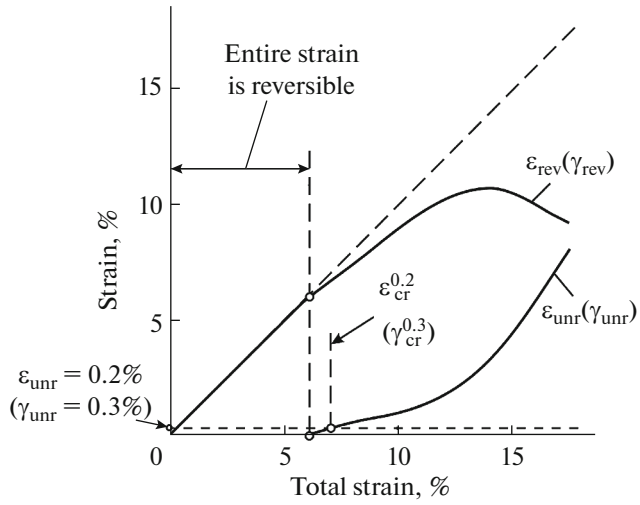

Fig. 3. Determination of critical strains $\varepsilon_{cr}^{0.2}$ and $\gamma_{cr}^{0.3}$ in SMAs; ε_{rev} (γ_{rev}) is the strain reversible on unloading and on heating, ε_{unr} (γ_{unr}) is unrecovered strain.

tional yield strength ($\tau_{0.3}$) determined with respect to this transition are not related to the accumulation of unrecovered strain by slip mechanisms; therefore, they are not the mechanical characteristics that determine the limiting allowable alloy loading conditions. When reaching τ_m, a relatively insignificant increase in stresses causes a significant increase in the strains (then, it can be recovered upon the reverse martensitic transformation). In the third segment, the slopes of the τ–γ curve increases, which is due to exhausting of the martensitic transformation and stress twinning and to material forming by predominantly slip mechanisms.

The shape recovery curves measured after deformation of the alloys at 5°C were used to determine the strain dependences of the temperatures of the onset (A_s^r) and finish (A_f^r) shape recovery (Fig. 2). The shape recovery temperature increases with the strain and the interval A_s^r–A_f^r is expanded. For alloy 2, this interval is 5–7°C at $\gamma < 6\%$ and 12–15°C at $\gamma > 6\%$. Alloy 1 is characterized by a wider interval of shape recovery temperatures: it is ≈10°C at $\gamma = 2\%$. The extrapolation of the dependences of the shape recovery temperatures enables the conclusion that the reverse martensitic transformation temperature (A_s, A_f) of these alloys lie in the range from 20°C to 35°C.

To estimate the working capacity of SME constructions, the total strain to which unrecovered strain $\varepsilon_{unr} = 0.2\%$ (for tensile/compression and bending strain) or $\gamma_{unr} = 0.3\%$ (for torsion) corresponds should be used as the limiting allowable (critical) strain value. An unrecovered strain of 0.2–0.3% is within the tolerances for majority of products and can be quite correctly measured during tests. We denote this critical degree of strain as $\varepsilon_{cr}^{0.2}$ or $\gamma_{cr}^{0.3}$ (Fig. 3). If the total strain is not higher than the critical strain, it should be completely reversible; i.e., it should be removed on unloading and be recovered during subsequent heating. In this case, we have to take into account the dependence of the critical strain on the test temperature.

In the alloys, the value of $\gamma_{cr}^{0.3}$ decreases as the test temperature increases (Fig. 4a). Alloy 1 has the best deformation characteristics in the temperature range 5–20°C. However, it begins to give way to alloy 2 with a higher nickel content as temperature increases, in particular, in the case of an unrecrystallized structure. To explain this fact, it is necessary to introduce another characteristic, namely, limiting allowable (critical) stress τ_{cr} corresponding to strain $\gamma_{cr}^{0.3}$. As is seen from Fig. 4a, $\gamma_{cr}^{0.3}$ = const at temperatures of 5–20°C. In alloy 1 subjected to recrystallized annealing, we have $\gamma_{cr}^{0.3} = 12 \pm 0.6\%$ and, in alloy 2, $\gamma_{cr}^{0.3} = 10.5 \pm 0.4\%$. The critical stresses corresponding to these strains (at temperatures from 5 to 20°C) are 300 ± 20 and 420 ± 15 MPa, respectively (Fig. 4b). Since the structures of the alloys are martensitic in the case of

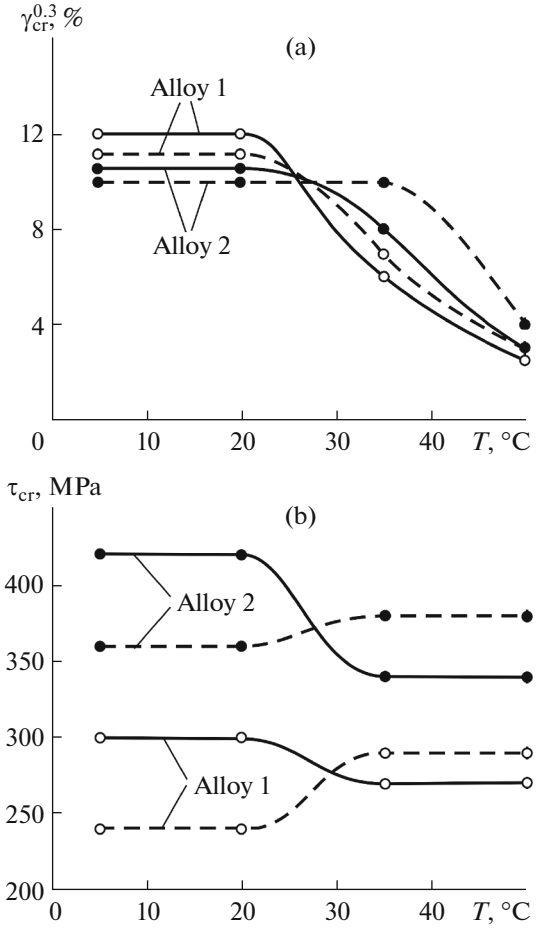

Fig. 4. Temperature dependences of (a) critical strains and (b) critical stresses in titanium nickelide-based alloys with (solid lines) recrystallized and (dashed lines) unrecrystallized structures.

strain by 10–12% at temperatures 5–20°C [6, 15], we can state that $\tau_{cr} = 300$ MPa and $\tau_{cr} = 420$ MPa are the stresses that cause slip in martensite in alloys 1 and 2, respectively.

The structures of both alloys in the recrystallized state contain the *B*2 phase in the unloaded state at temperatures 35–50°C. On loading, material forming occurs via the martensitic mechanism until the slip stress is reached in the *B*2 phase. Then forming occurs via a mixed mechanism (simultaneously by slip and the martensitic transformation); i.e., an unrecovered strain should appear. In alloy 2, we have $\gamma_{cr}^{0.3} = 8 \pm 0.3\%$ at 35°C and $\gamma_{cr}^{0.3} = 3 \pm 0.5\%$ at 50°C, and τ_{cr} corresponding to these values is 340 ± 10 MPa. It can be stated that this stress is the slip stress in the *B*2 phase. We can also state in the same procedure that the slip stresses in the *B*2 phase of alloy 1are 270 ± 15 MPa; i.e., slip in the recrystallized *B*2 phase is developed at lower stresses than in martensite. The specimens of both alloys that were not subjected to recrystallization annealing demonstrate the opposite situation: slip processes in martensite are developed at lower stresses than in the *B*2 phase due to a highly imperfect structure.

The obtained temperature dependences of the critical strain can be explained by the influence of the alloy structure on the martensitic transformation mechanisms and on the slip mechanisms. The value of $\gamma_{cr}^{0.3}$ is determined by the relation between the martensitic transformation and/or twinning stresses and/the stresses at which the slip processes (τ_{cr}) begin to develop in the alloy matrix. In this case, it should be taken into account that the martensitic transformation stresses increase as compared to the initial martensitic shear stress (τ_m) during deformation of the alloy. The character of change in these stresses is dependent on the test temperature, the chemical composition, and the structure of the alloy and determines the τ–γ diagram shape at the end (Fig. 1). The accumulation of unrecovered strain begins at the moment when the stresses required for the development of the martensitic transformation and twinning reach τ_{cr}. The higher temperature, the higher the martensitic transformation stresses and the sooner the critical stresses.

In alloy 2 with a high nickel content, the volume fraction of disperse particles of Ti_3Ni_4 intermetalic compound, which precipitate during aging, is larger than that in alloy 1 [15]. These particles strengthen the alloy matrix; therefore, the critical stresses τ_{cr} corresponding to the onset of slip processes in martensite *B*19' or *B*2 austenite in alloy 2 are higher than those in alloy 1. Despite this fact, alloy 1 with a lower nickel content is characterized by higher values of $\gamma_{cr}^{0.3}$ at low deformation temperatures. This is due to that the martensite shear stresses in alloy 1 are lower than the stresses in alloy 2, and, therefore, reach the critical values at higher strains. However, the martensitic shear stress increases with the test temperature. In this case, the rate of increase of stress is such that the critical stresses in alloy 1 are reached earlier than in alloy 2 upon deformation in the temperature range 35–50°C.

The highest effect of the matrix strengthening is observed in aging of alloy 2 without previous recrystallized annealing. A large number of defects of the crystal structure and a large volume fraction of disperse Ti_3Ni_4 particles substantially hamper slip in the *B*2 phase and provide the highest critical deformations in the alloy in the superelastic state (at test temperatures 35–50°C).

Consider the properties of the alloys with an unrecrystallized structure. The structure formed during aging without previous recrystallization annealing is characterized by a higher density of defects (first, dislocations). The existence of the fields of elastic stresses around the pile-up of dislocations and chemical microheterogeneities decreases the uniformity of the

distribution of intermetalic compounds precipitated during aging [16], which influences the level of the critical stresses and strains. The tests of the specimens at temperatures lower than A_s (from 5 to 20°C) demonstrate a lower level of the critical stresses τ_{cr}. For example, in alloys 1 and 2 with the recrystallized structure in the martensitic state, $\tau_{cr} = 300 \pm 20$ and 420 ± 15, respectively, and in alloys which were not subjected to the recrystallization annealing, $\tau_{cr} = 240 \pm 10$ and 360 ± 10 MPa (Fig. 4). The development of slip at lower applied stresses can be due to a high level of internal stresses, which occur in martensite *B*19' because of a high defect concentration, the existence of chemical microheterogeneities, and a high volume fraction of disperse Ti_3Ni_4 particles. These stresses are added to external stresses. A decrease in τ_{cr} leads to a slight decrease in the value of $\gamma_{cr}^{0.3}$: to $11 \pm 0.4\%$ in alloy 1 and to $10 \pm 0.3\%$ in alloy 2.

The value of τ_{cr} of alloy 2 in the temperature interval higher than A_f (35–50°C) increases to 380 ± 20 MPa as a result of strengthening the *B*2 phase related to an increased defect density. This is accompanied by the increase in $\gamma_{cr}^{0.3}$ to $10 \pm 0.5\%$ at 35°C and to $4 \pm 0.3\%$ at 50°C. Similar change in the critical stresses and strains in the temperature range 35–50°C is observed in alloy 1 as well, but it is less pronounced ($\tau_{cr} = 290 \pm 10$ MPa, $\gamma_{cr}^{0.3} = 7 \pm 0.3\%$ at 35°C, $\gamma_{cr}^{0.3} = 3 \pm 0.2\%$ at 50°C).

The deformation schemes upon the tests substantially influence the deformation characteristics. Figure 5 shows the temperature dependences of critical strain $\varepsilon_{cr}^{0.2}$ built on the results of the bending and tensile tests of the specimens with a recrystallized structure. The tension is the least favorable deformation scheme upon the deformation of alloys in a "plastic" state (at 5–20°C). This fact can be explained by that the tensile stresses and tensile strains are uniformly distributed over the specimen cross-section and the measured average strain is maximal. At the same time, the maximum bending and torsion strains appeared on the specimen surface are substantially higher than the values averaged over the cross-section. Thus, if a mixed deformation mechanism (martensitic transformation + slip) is observed on the surfaces of specimens subjected to bending or torsion, the mechanisms of elastic deformation and martensitic transformation can still dominate in internal layers of the specimens. The absence of slip in the internal volumes of the specimen would determine complete recovery of the macroscopic deformation during subsequent unloading and heating at high values of $\gamma_{cr}^{0.3}$ ($\varepsilon_{cr}^{0.2}$) as compared to tension. The influence of a loading scheme on the critical strains can also be explained by the anisotropy of the crystallogeometric characteristics of the $B2 \rightarrow B19'$ martensitic transformation and

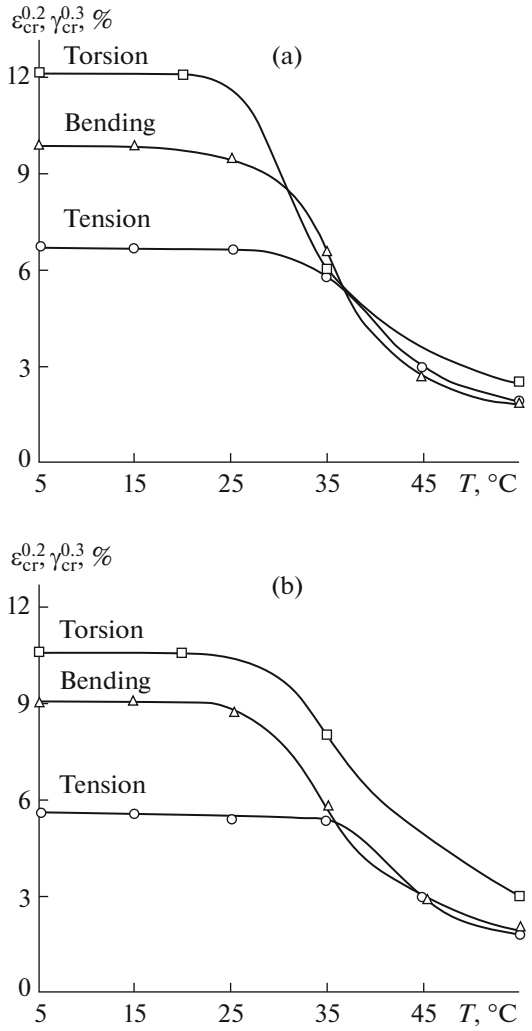

Fig. 5. Effect of a deformation scheme on the temperature dependence of the critical strains for alloys (a) 1 and (b) 2 with the recrystallized structures.

by the fact that the torsion causes a stress–strain state, which is closest to the scheme that occurs upon the crystallographic shift during the martensitic transformation [16].

In the superelastic state (at 35–50°C), the influence of a loading scheme on the critical strains in alloy 2 is weaker as compared to that in the low-temperature state, and the critical strains in alloy 1 are only slightly dependent on the loading scheme and reach comparable values. It should be noted that the obtained results are preliminary, and the influence of the scheme of the stress–strain state on the temperature dependences of the critical strain needs a further detailed study.

CONCLUSIONS

The critical strains and stresses are important parameters, which characterize the working ability of

SMA, since the excess of these values leads to degeneration of the shape recovery characteristics. The results of the studies showed that the stress–strain characteristics of titanium nickelide SMAs are substantially dependent on the chemical composition and the structural state of the *B*2 matrix and the thermomechanical treatment conditions. Bending and torsion are the most favorable deformation schemes for the alloys in the martensite state, and tension is the least favorable scheme. The critical degrees of strain upon bending, tension, and torsion are quite close to each other in the case of deformation in the superelastic state.

In this work, the critical stresses and strains were determined on loading the alloys under isothermal conditions. At the same time, some constructions, in which SMAs are used, operate in athermal conditions, when strain accumulation recovery occurs during thermal cycling through the interval of the forward and reverse martensitic transformation. In this case, some regularities of the martensitic transformation and slip mechanisms and the influences of the chemical composition and the alloy structure can differ from those observed under isothermal conditions.

The established regularities of changing the critical stresses and strains should be taken into account in the engineering calculations of SME parts. In particular, the temperature dependences of the critical strains were used at AO KIMPF (Moscow, Russia) in the development of the technology of applying, calculations of design, and optimization of fabricating implants from titanium nickelide-based alloys for neurosurgery, traumatology, and orthopedics.

ACKNOWLEDGMENTS

This work was performed in the framework of the base part of state task for the higher school no. 11.7449.2017/BCh using the equipment of the Resource Collective Use Center Aviation-Space Materials and Technologies at the Moscow Aviation Institute.

REFERENCES

1. K. Otsuka and X. Ren, "Physical metallurgy of Ti–Ni-based shape memory alloys," Progr. Mater. Sci. **50** (5), 511–678 (2005).
2. S. A. Shabolovskaya, "Surface, corrosion, and biocompatibility aspects of Nitinol as an implant material," Bio-Medical Mater. and Eng., No. 12, 69–109 (2002).
3. M. S. Blanter, I. S. Golovin, H. Neuhäuser, and H.-R. Sinning, *Internal Friction in Metallic Materials* (Springer-Verlag, Berlin Heidelberg, 2007).
4. I. Yoshida and S. Yoshida, "Damping capacity of Ti–Ni shape memory alloys," Solid State Phenomena **89**, 315–320 (2003).
5. K. Ootsuka, K. Simidzu, Yu. Simidzu, et al., *Shape Memory Alloys*, Ed. by Kh. Funakubo (Metallurgy, Moscow, 1990).
6. A. A. Il'in, M. Yu. Kollerov, V. I. Khachin, and D. E. Gusev, "Medical instruments and implants of titanium nickelide: physical metallurgy, technology, and application," Rus. Met. (Metally), No. 3, 296–300 (2002).
7. V. E. Gyunter, V. N. Khodorenko, Yu. F. Yasenchuk, et al., Titanium Nickelide. *New-Generation Medical Material* (MITs, Tomsk, 2006).
8. V. N. Khachin, V. G. Pushin, and V. V. Kondrat'ev, *Titanium Nickelide* (Nauka, Moscow, 1992).
9. A. A. Il'in, M. Yu. Kollerov, A. A. Shinaev, and I. S. Golovin, "Mechanisms of forming upon deformation and heating of titanium shape memory alloys," Metalloved. Term. Obrab. Met., No. 4, 12–16 (1998).
10. M. Yu. Kollerov, D. E. Gusev, A. A. Sharonov, and E. V. Shinaeva, "Structural mechanism of controlling characteristics of shape memory of titanium nickelide–based alloys," Deform. Razrush. Mater., No. 2, 20–25 (2016).
11. M. Yu. Kollerov, D. E. Gusev, A. V. Burnaev, and A. A. Sharonov, "Effect of the chemical composition and the structure on the thermomechanical behavior of titanium nickelide–based alloys," Metalloved. Term. Obrab. Met. **744**, (6), 38–44 (2017).
12. *ASTM F2082/F2082M-16. Standard Test Method for Determination of Transformation Temperature of Nickel–Titanium Shape Memory Alloys by Bend and Free Recovery.* https://www.astm.org / Standards / F2082.htm.
13. M. Yu. Kollerov, D. E. Gusev, G. V. Gurtovaya, et al., *Functional Shape Memory Materials: A Textbook* (INFRA-M, Moscow, 2016).
14. V. A. Lobodyuk and E. I. Estrin, *Martensitic Transformations* (Fizmatgiz, Moscow, 2009).
15. M. Yu. Kollerov, A. A. Il'in, I. S. Pol'kin, A. S. Fainbron, D. E. Gusev, and S. V. Khachin, "Structural aspects of the manufacture of semiproducts made from titanium nickelide–based alloys," Rus. Met. (Metally), No. 5, 408–414 (2007).
16. A. A. Il'in, *Mechanism and Kinetics of Phase and Structural Transformations in Titanium Alloys* (Nauka, Moscow, 1994).

Translated by Yu. Ryzhkov